

RESEARCH

Open Access



Synthesis and antitumor activity of dolutegravir derivatives bearing 1,2,3-triazole moieties

Xixi Hou^{1†}, Longfei Mao^{2,3*†}, Yajie Guo^{4†}, Lan Wang², Lizeng Peng⁵, Huili Wang⁶, Jianxue Yang^{1*}, Sanqiang Li^{2*} and Yue-Ming Li^{3*}

Abstract

Modification of marketed drugs is an important way to develop drugs because its safety and clinical applicability. Oxygen-nitrogen heterocycles are a class of important active substances discovered in the process of new drug development. Dolutegravir, an HIV drug with a nitrogen-oxygen heterocycle structure, has the potential ability to inhibit cell survival. In order to find and explore novel anti-tumor drugs, new dolutegravir derivatives bearing different 1,2,3-triazole moieties were prepared via click reactions. In vitro biological experiments performed in several lung cancer cell lines suggested that these novel compounds displayed potent anti-tumor ability. Especially, the compound 9e with a substituent of 2-methyl-3-nitrophenyl and the compound 9p with a substituent of 3-trifluoromethylphenyl were effective against PC-9 cell line with IC₅₀ values of 3.83 and 3.17 μM, respectively. Moreover, compounds 9e and 9p were effective against H460 and A549 cells. Further studies suggested that compounds 9e and 9p could induce cancer cell apoptosis in PC-9 and H460, inhibit cancer cell proliferation, change the cell cycle, and increase the level of reactive oxygen species (ROS) which further induce tumor cell apoptosis. In addition, compounds 9e and 9p increased LC3 protein expression which was the key regulator in autophagy signaling pathway in PC-9 cells. Compound 9e also showed low toxicity against normal cells, and could be regarded as an interesting lead compound for further structure optimization.

Keywords Dolutegravir, 1, 2, 3-triazole, Synthesis, Antitumor, Autophagy

[†]Xi-xi Hou, Long-fei Mao and Yajie Guo have contributed equally to this work as first co-authors.

*Correspondence:

Longfei Mao
longfeimao1988@163.com
Jianxue Yang
Docyjx@126.com
Sanqiang Li
sanqiangli2001@163.com
Yue-Ming Li
ymli@nankai.edu.cn

¹Department of Pharmacy, The First Affiliated Hospital, and College of Clinical Medicine of Henan University of Science and Technology, Luoyang 471003, China

²College of Basic Medicine and Forensic Medicine, Henan University of Science and Technology, 263 Kaiyuan Road, Luoyang 471003, China

³State Key Laboratory of Medicinal Chemical Biology, College of Pharmacy and Tianjin Key Laboratory of Molecular Drug Research, Nankai University, Haihe Education Park, 38 Tongyan Road, Tianjin 300350, China

⁴Department of Emergency, The Eighth Affiliated Hospital, Sun Yat-Sen University, Shenzhen 518033, China

⁵Institute of Agro-Food Science and Technology, Key Laboratory of Agro-Products Processing Technology of Shandong Province, Key Laboratory of Novel Food Resources Processing Ministry of Agriculture, Shandong Academy of Agricultural Sciences, Jinan 250100, China

⁶University of North Carolina Hospitals, 101 Manning Dr, Chapel Hill, Orange County, NC 27599, USA



© The Author(s) 2024. **Open Access** This article is licensed under a Creative Commons Attribution 4.0 International License, which permits use, sharing, adaptation, distribution and reproduction in any medium or format, as long as you give appropriate credit to the original author(s) and the source, provide a link to the Creative Commons licence, and indicate if changes were made. The images or other third party material in this article are included in the article's Creative Commons licence, unless indicated otherwise in a credit line to the material. If material is not included in the article's Creative Commons licence and your intended use is not permitted by statutory regulation or exceeds the permitted use, you will need to obtain permission directly from the copyright holder. To view a copy of this licence, visit <http://creativecommons.org/licenses/by/4.0/>. The Creative Commons Public Domain Dedication waiver (<http://creativecommons.org/publicdomain/zero/1.0/>) applies to the data made available in this article, unless otherwise stated in a credit line to the data.

Introduction

Lung cancer is the leading cause of cancer-related deaths globally, posing a serious threat to human health [1]. Drug therapy is a crucial approach in the treatment of lung cancer, but traditional drugs often result in severe side effects and drug resistance. Therefore, the development of new lung cancer drugs aimed at reducing treatment side effects and resistance is essential. This effort aims to enhance treatment tolerability, ultimately improving the quality of life for patients. Such advancements carry significant societal significance and economic value [2]. Over the years, endeavors have focused on discovering drugs that either provide superior alternatives to existing standards or introduce entirely novel mechanisms of action. Despite the progress in antitumor drug development, an ongoing imperative exists to uncover and design agents that are not only safer but also more effective, minimizing side effects and mitigating drug resistance. The modification of marketed drugs is an important way to develop drugs because this approach ensures both safety and clinical applicability.

Human immunodeficiency virus (HIV) is a lentivirus that infects cells of the human immune system. By damaging the body's immune system, the virus causes a variety of diseases including cancer, and ultimately threatens the lives of patients [3, 4]. After a patient is infected with HIV, the virus cannot be completely eliminated from the body, and one can only rely on drug treatments to reduce the viral load in body. With the effective treatment of antiretroviral virus, AIDS-related opportunistic infections have been effectively controlled. However, with the prolongation of disease courses, malignant tumors have become the main cause of death in affected individuals [5, 6]. In patients with HIV infections, cancers exhibit accelerated growth and heightened aggressiveness. Studies showed that, comparing with the general population, people infected with HIV are 500 times more likely to be diagnosed with Kaposi sarcoma, 12 times more likely to be diagnosed with non-Hodgkins lymphoma, and, among women, 3 times more likely to be diagnosed with cervical cancer [7, 8]. It would be of high interest to develop new agents which could effectively suppress the HIV infection

or HIV replication on one hand, and could significantly inhibit the growth of tumor cells on the other [9].

HIV integrase inhibitors are an important class of anti-AIDS drugs, and can effectively inhibit the replication process of retrovirus and block the integration of virus DNA into the host chromosome DNA [10]. It would be possible to develop new agents exhibiting both the antiviral and antitumor activities by introduction of new functional groups into such anti-HIV agents. One can also take the advantages such as safety or the pharmacokinetic issues of a clinically used drug when using known drug as a starting point [11, 12].

Dolutegravir (DTG), as a class of HIV integrase inhibitors approved by FDA priority [13], has shown strong antiviral and anti drug-resistant properties [14]. In the treatment of patients with first-time HIV infection, DTG taken once a day is comparable to that of Raltegravir (RAL) taken twice a day. The results of preclinical study shows that DTG has little toxicity, and no obvious fertility toxicity or teratogenic toxicity was found when the dose of DTG was 27 times greater than the clinical dose [15]. The results of clinical studies shows that DTG is better than control drug in the treatment of HIV first-infected people and has better effect on the patients who failed treatment without use of integrase inhibitors. Good responses were also found in adult patients who were resistant to RAL or EVG [16] (Fig. 1).

Oxygen-nitrogen heterocycles are a class of important active substances discovered in the process of new drug development. And DTG is a drug with a nitrogen-oxygen heterocycle structure. The outstanding performance of DTG in the treatment of HIV infections made it an ideal starting point for the development of new chemical entities which would be expected to show both antiviral and antitumor activity. In our previous report we showed that introducing 1,2,3-triazole moiety to dolutegravir produced a new dolutegravir derivative which could inhibit proliferation and induce apoptosis of non-small cell lung cancer cells via calcium signaling pathway [17]. Encouraged by this preliminary result, we wish to further study the possibility of using dolutegravir derivatives as new antitumor agents.

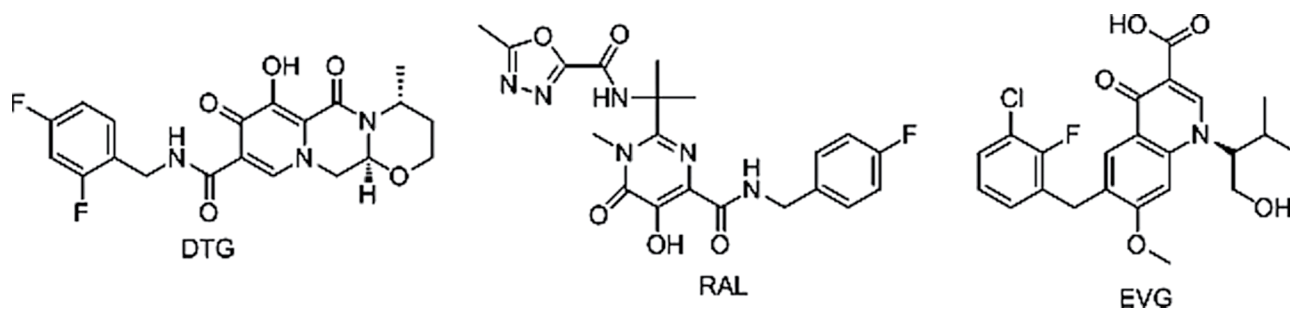


Fig. 1 The structures of DTG, RAL and EVG

As an important class of nitrogen-containing heterocyclic compounds, 1,2,3-triazoles can be easily, efficiently and quickly prepared by click reaction [18]. The unique features of such heterocycles made them ideal functional groups for the modification of a known drug, or as structural surrogates for other functional groups in a known drug [19–22]. Previous studies have found effective anti-tumor abilities by combining 1,2,3-triazoles with marketed drugs include icotinib, zidovudine, and pomadomide [23, 24]. Based on our previous research focusing on the synthesis of 1,2,3-triazole analogues with known drugs, which exhibited promising anticancer activity, we sought to explore the antitumor activity of dolutegravir and 1,2,3-triazoles combination. In this regard, a series of 1,2,3-triazole derivatives were designed and prepared using dolutegravir as the parent nucleus according to the principle of bioactive substructure splicing. Subsequently, comprehensive evaluations of their biological activity especially the antitumor activity against lung cancer cell lines were measured. The aim of our study is to discover more efficient anticancer agents for treating lung cancer.

Results and discussion

The preparation of the target products started from commercially available methyl 4-methoxyacetate (1). Condensation of 1 with DMF-DME gave compound 2 which reacted with aminoacetaldehyde dimethyl acetal to give compound 3. Compound 3 reacts with dimethyl oxalate to produce an reaction intermediate under room temperature conditions, and then undergoes cyclization under heating conditions to yield compound 4. Partial hydrolysis of 4 with lithium hydroxide gave carboxylic acid 5 which was further hydrolyzed with HCOOH to give 6. Reaction of 6 with (*R*)-3 aminobutanol gave compound 7 which was converted to compound 8 using HATU/DIPEA as the coupling agent. Click reaction of 8 with azide compounds bearing different substituents furnished the synthesis of target compounds 9 and 10 (Scheme 1 and Table 1). The structures of the target compounds were confirmed with ^1H and ^{13}C nuclear magnetic resonance spectroscopy.

Compounds 9 and 10 suppressed cancer cell viability

At first, CCK8 assay was carried out to evaluate the anti-proliferative activity of dolutegravir-1,2,3-triazole derivatives against different cancer cell lines. The results of cell viability of three lung cancer cell lines A549, PC-9 and H460 in the presence of compounds 9 and 10 are summarized in Table 2. Cells were treated with different compounds at the concentration of 20 μM for 48 h. Preliminary results suggested that most of the compounds exhibited strong effects on lung cancer cell lines H460 and PC-9 and weak effects on A549.

Based on these preliminary results, compounds 9c, 9e, 9f, 9i, 9k, 9 L, 9p, 9q, 9t, 9u, 9v, 9w, 10c, 10e which were effective to most of the cell lines were chosen for the measurement of the half-maximal inhibitory concentration (IC_{50}). The results are given in Table 3. As shown in Table 3, compounds 9e and 9p gave promising inhibitory activities against A549, PC-9 and H460 cell lines with IC_{50} values of 8.72 ± 0.11 and 12.97 ± 0.32 , 3.83 ± 0.73 and 3.17 ± 0.18 , 11.76 ± 2.31 and $10.69 \pm 0.48 \mu\text{M}$, respectively. HRM (Human Renal Mesangial) cell line was used as a control to study the toxicity of these compounds against normal human cells. We discovered compounds that exhibit inhibitory effects on lung cancer cells, with good safety profiles in HRM cells; the half-maximal inhibitory concentration is generally greater than 50 μM .

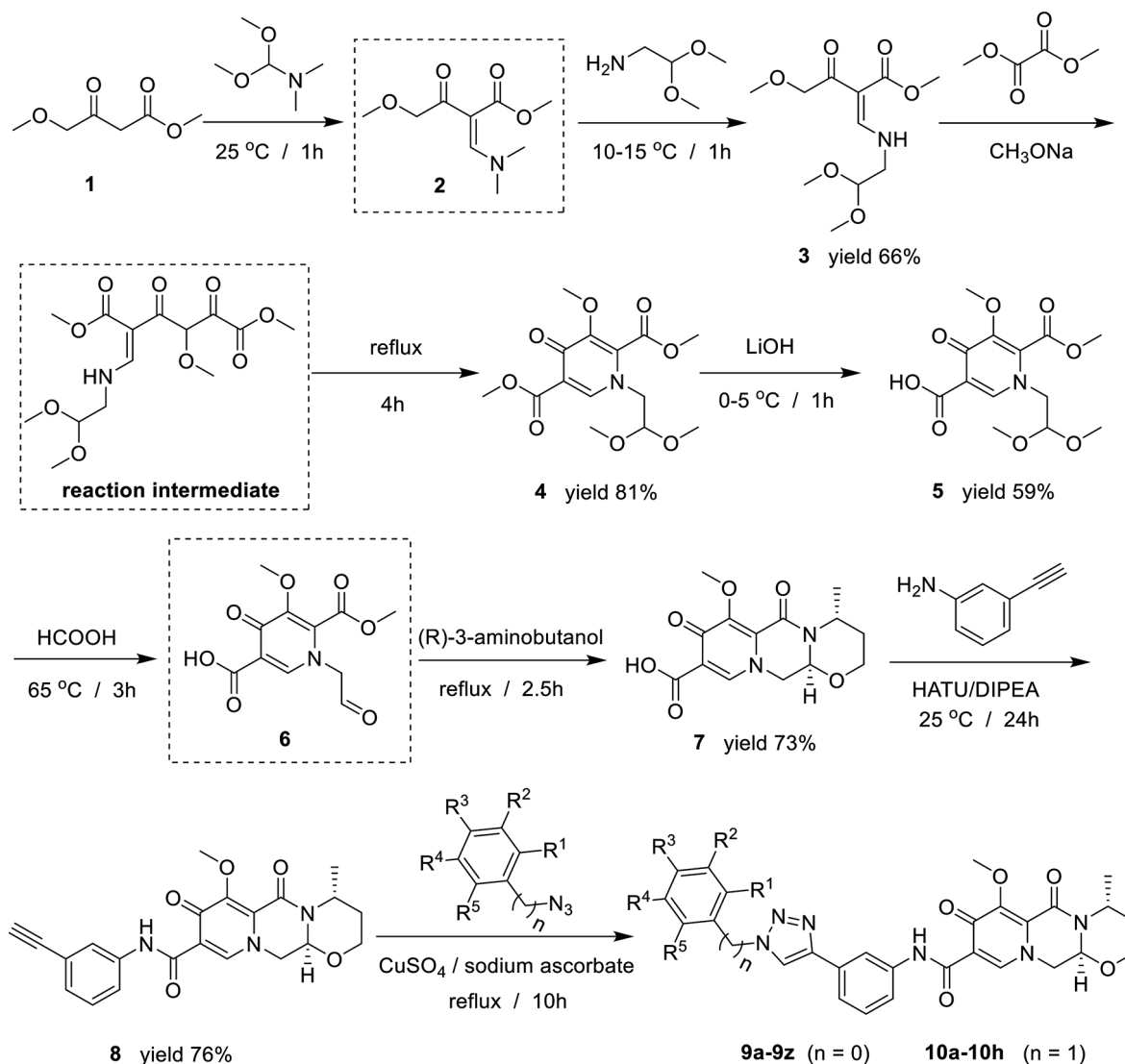
Inhibition of cancer cell proliferation by compounds 9e and 9p

LIVE/DEAD staining experiments were carried out to evaluate the anti-proliferative activity of dolutegravir derivatives 9e and 9p against PC-9 and H460 cell lines. The tumor cells were treated with 5 μM , 10 μM or 20 μM of 9e and 9p for 24 h. The live and dead cells were photographed and counted. The results are given in Fig. 2. As shown in Fig. 2, the number of live cells of PC-9 decreased significantly in a dose dependent manner after being treated with 9e. The ratio of dead/live cells was also increased significantly with the increase of concentration (Fig. 2A). In the case of 9p, the number of live cells of PC-9 also decreased with the increase of concentration (Fig. 2A). The ratio of dead/live cells was increased compared with untreated group but not completely in a dose dependent manner (Fig. 2A). The possible reason was that at the concentration of 20 μM , cell proliferation was largely suppressed, resulting in few living cells remaining. Similar results were observed in H460 cells after being treated with 9e or 9p (Fig. 2B).

The plate clone formation experiments were also carried out to further confirm the effects of dolutegravir derivatives on cell proliferation. Compounds 9e and 9p with different concentrations (0, 2, 4, 8, 16 and 32 μM) were added to the cells. Preliminary results suggested that 9e and 9p showed anti-proliferative activity against cell lines PC9 and H460 in a dose-dependent manner (Fig. 2C).

Influences of 9e and 9p on the apoptosis of cancer cells

Further, the effects of 9e and 9p on the apoptosis of tumor cells were studied to get details of the suppression of cell proliferation caused by these compounds. PC-9 and H460 cells treated with different concentrations of 9e or 9p were stained with Annexin V-FITC and PI, and the numbers of apoptosis cells were analyzed by the flow cytometry. The results are given in Fig. 3. As illustrated



Scheme 1 Preparation of compounds 9 and 10

in Fig. 3, for PC-9 cells, both 9e and 9p exhibited significant effects on cell apoptosis at the concentration of 8 μM , while little influence at the concentrations of 2 μM or 4 μM (Fig. 3A). H460 cells that treated with 8 μM and 16 μM of 9e showed significant increased apoptosis (Fig. 3B). Moreover, compound 9p at concentrations of 4 μM , 8 μM and 16 μM significantly increased apoptosis of H460 cells (Fig. 3B).

Influences of 9e and 9p on the cell cycles of cancer cells

Cancer cell lines PC-9 and H460 were then treated for 48 h with 9e or 9p at different concentrations to investigate the effects of these compounds on regulating the cell cycle. Cell cycle distributions were analyzed using the flow cytometry technique. The results are given in Fig. 4. As shown, for PC-9 cells, 4 μM of 9e treatment had moderate effects on cell cycle while 8 μM of 9e decreased

G0/G1 phase and increased S and G2/M phase (Fig. 4A). Compound 9p at the concentrations of 4 μM and 8 μM all induced an S and G2/M cell cycle arrest, as demonstrated by the decreased G0/G1 and increased S and G2/M phase (Fig. 4A). For H460 cells, 9e treatment increased G2/M phase and had little influences on G0/G1 or S phase (Fig. 4B). Compound 9p could significantly decrease the S phase compared with untreated cells (Fig. 4B).

Compounds 9e and 9p triggered reactive oxygen species generation in tumor cell lines

Reactive oxygen species could induce cell death and suppress cell growth and proliferation [25, 26]. To assess the role of compounds 9e and 9p in ROS generation, different cancer cell lines were treated with 9e or 9p for 24 h. DCFDA was used to stain cells and ROS was detected with fluorescent microscope. The results are given in

Table 1 R-group of compounds 9 and 10

Compd no.	n	R ¹	R ²	R ³	R ⁴	R ⁵
9a	0	F	H	H	H	H
9b	0	OCH ₃	H	NO ₂	H	H
9c	0	CF ₃	H	H	H	H
9d	0	H	H	CF ₃	H	H
9e	0	CH ₃	NO ₂	H	H	H
9f	0	H	CH ₃	H	H	H
9g	0	H	H	F	H	H
9h	0	H	H	OCH ₂ CH ₃	H	H
9i	0	OCF ₃	H	H	H	H
9j	0	H	OCH ₃	OCH ₃	H	H
9k	0	CH ₂ CH ₃	H	H	H	H
9L	0	H	OCH ₃	H	H	H
9m	0	H	H	CH ₂ CH ₃	H	H
9n	0	H	H	C(CH ₃) ₃	H	H
9o	0	H	H	H	H	H
9p	0	H	CF ₃	H	H	H
9q	0	CF ₃	H	H	CF ₃	H
9r	0	H	CF ₃	H	CF ₃	H
9s	0	CH ₃	H	H	H	H
9t	0	OCH ₃	H	H	H	H
9u	0	Br	H	H	H	H
9v	0	Cl	H	H	H	H
9w	0	I	H	H	H	H
9s	0	H	H	OCH ₃	H	H
9y	0	H	H	CH ₃	H	H
9z	0	CH ₃	H	CH ₃	H	CH ₃
10a	1	H	Br	H	Br	H
10b	1	H	H	H	H	H
10c	1	Br	H	H	H	H
10d	1	H	OCH ₃	H	H	H
10e	1	H	Br	H	H	H
10f	1	F	H	H	H	H
10g	1	CH ₃	H	H	H	H
10h	1	CF ₃	H	H	H	H

Fig. 5. As observed in Fig. 5, ROS generation was significantly increased when PC-9 and H460 cell lines were treated with 9e or 9p.

Autophagy signalling pathway was stimulated by 9e and 9p

To determine the role of compounds 9e and 9p on regulating the development of cell proliferation, expressions of key proteins which were involved in cell growth progresses such as autophagy, apoptosis, cell cycle and DNA damage were examined. The results are summarized in Fig. 6. Ubiquitin like molecule light chain 3 (LC3) is a key marker of autophagy. Our preliminary study suggested that the expression of LC3 was significantly increased when PC-9 was treated with 9e or 9p. Caspase3, which is one of the key proteins in regulating apoptosis, however, was not changed in tumor cells after treated with 9e or 9p. Cell cycle regulation proteins such as CyclinD,

CyclinE or β -catenin were also not affected when PC-9 was treated with 9e or 9p. Further, H2AX variant histone (γ -H2AX), which was responsible for DNA damage, was also not affected when PC-9 were treated with 9e or 9p.

Conclusions

In summary, we have shown that conventional click reactions between dolutegravir and different azides provided derivatives bearing different 1,2,3-triazole moieties. These compounds exhibited interesting anti-tumor activities. Especially, compounds 9e and 9p were active against PC9 with IC₅₀ values of 3.83 and 3.17 μ M, respectively. Further study showed that these two compounds could induce apoptosis in PC-9 and H460 cells, inhibit tumor cell clone formation, and increase the level of reactive oxygen species (ROS) to further stimulate tumor cell apoptosis. These two compounds could also activate the LC3 signaling pathway to induce autophagy in PC-9

Table 2 Inhibition performance of selected tumor cell lines by the compounds 9 and 10

Compd no.	Cell viability (100%), 20 μ M, 48 h		
	A549	PC9	H460
9a	95.90	52.03	47.20
9b	92.60	104.86	98.64
9c	9.48	13.91	32.97
9d	82.37	105.15	69.71
9e	9.14	24.05	30.94
9f	33.47	8.80	39.20
9g	91.65	88.64	97.85
9h	77.55	71.96	52.87
9i	17.41	18.95	8.52
9j	87.42	85.93	92.89
9k	83.48	23.40	18.72
9L	73.36	47.77	20.32
9m	65.08	63.65	62.63
9n	67.60	59.44	24.58
9o	78.59	94.56	87.72
9p	10.85	2.11	5.63
9q	54.85	18.17	17.63
9r	90.73	98.55	117.07
9s	82.07	65.73	48.37
9t	7.32	4.56	3.27
9u	64.09	43.88	31.00
9v	54.06	47.42	38.13
9w	57.94	55.21	30.63
9x	69.21	78.11	108.05
9y	85.43	79.67	94.78
9z	91.32	73.07	55.57
10a	87.40	103.57	82.32
10b	87.18	96.85	55.00
10c	68.05	50.54	41.79
10d	89.00	83.17	77.21
10e	96.13	49.85	28.88
10f	82.22	61.10	32.43
10g	71.58	54.61	35.98
10h	77.72	66.77	28.10
DTG	108.82	91.66	27.24

Different cells were treated with 20 μ M compounds and DTG. After 48 h treatment, cell viability was measured using a CCK8 assay kit. Data are presented as mean \pm SE

* $P < 0.05$

cells. Compound 9e also showed low toxicity against normal cells. The easy availability, the promising bioactivity against tumor cells and the relatively low toxicity of the compounds against normal cells made them ideal leads for further structure optimization.

Experimental

Materials and chemistry

All the reagents and solvents were obtained from commercially available sources. The ^1H NMR and ^{13}C NMR spectra were acquired in a DMSO- d_6 solution using a Bruker 400 MHz or 600 MHz NMR spectrometer.

Table 3 The half-maximal inhibitory concentration (IC_{50}) of the chosen compounds

Compd no.	IC_{50} (μ M), 48 h			
	A549	PC9	H460	HRM
9c	9.06 \pm 0.88	4.03 \pm 0.59	11.42 \pm 0.59	> 50
9e	8.72 \pm 0.11	3.83 \pm 0.73	11.76 \pm 2.31	> 50
9f	27.75 \pm 0.56	4.67 \pm 0.26	19.58 \pm 0.32	> 50
9i	11.06 \pm 1.07	4.53 \pm 0.31	8.24 \pm 2.06	> 50
9k	20.67 \pm 0.23	9.87 \pm 0.19	12.93 \pm 0.80	> 50
9L	44.34 \pm 1.21	9.20 \pm 0.65	25.48 \pm 0.43	43.29 \pm 3.27
9p	12.97 \pm 0.32	3.17 \pm 0.18	10.69 \pm 0.48	35.55 \pm 10.77
9q	13.63 \pm 1.79	6.78 \pm 0.31	16.50 \pm 0.57	> 50
9t	17.34 \pm 0.73	6.75 \pm 1.43	14.16 \pm 0.16	> 50
9u	> 50	7.77 \pm 0.37	37.32 \pm 2.25	> 50
9v	> 50	11.55 \pm 0.48	16.19 \pm 1.29	> 50
9w	33.66 \pm 0.68	9.94 \pm 0.36	14.71 \pm 2.83	> 50
10c	> 50	12.05 \pm 0.46	15.37 \pm 1.38	> 50
10e	> 50	10.12 \pm 0.71	9.44 \pm 1.53	> 50

Cells were treated with different concentrations of compounds (0, 0.5 μ M, 2 μ M, 8 μ M, 16 μ M, 32 μ M). After 48 h treatment, cell viability was measured using the CCK8 assay kit to calculate the inhibition percentage. Then the IC_{50} value was calculated using the GraphPad Prism software. Data are presented as mean \pm SE

* $P < 0.05$

Dolutegravir-1,2,3-triazole compounds was synthesized in-house. Dimethylsulfoxide (DMSO) was obtained from Sigma-Aldrich (St. Louis, Missouri, USA). Dulbecco's modified Eagle medium (DMEM), RPMI 1640 Medium, Fetal bovine serum (FBS) and penicillin/streptomycin were purchased from Gibco (Grand Island, NY, USA). Enhanced Cell Counting Kit-8, Calcein/PI Live/Dead Viability Assay Kit, Giemsa dye and Reactive Oxygen Species (ROS) Assay Kit were obtained from Beyotime Biotechnology (Shanghai, China). Annexin V-FITC/Propidium iodide (PI) staining kit and Matrigel Matrix were provided by BD Biosciences (Franklin Lake, New Jersey, USA).

Human lung cancer cell lines A549, PC-9 and H460 were all obtained from ATCC. Cells were cultured in DMEM or RPMI 1640 medium containing 10% FBS and 1% penicillin/streptomycin at 37 $^{\circ}\text{C}$ with a 5% CO_2 -humidified atmosphere.

Preparation of compounds 9 and 10

Synthesis of methyl (Z)-2-(((2,2-dimethoxyethyl)amino)methylene)-4-methoxy-3-oxobutanoate (3)

To methyl 4-methoxyacetoacetate (compound 1, 150 g, 1.0 mol) was added dropwise DMF-DMA (120 g, 1.0 mol) at room temperature in a period of 20 min. The color of the solution became black. The reaction temperature was maintained at 25 $^{\circ}\text{C}$, and the reaction mixture was stirred for 1 h. The course of the reaction was monitored with TLC. After the completion of the reaction, the reaction mixture was cooled to 10 to 15 $^{\circ}\text{C}$. Aminoacetaldehyde dimethylacetal (115 g, 1.1 mol) was

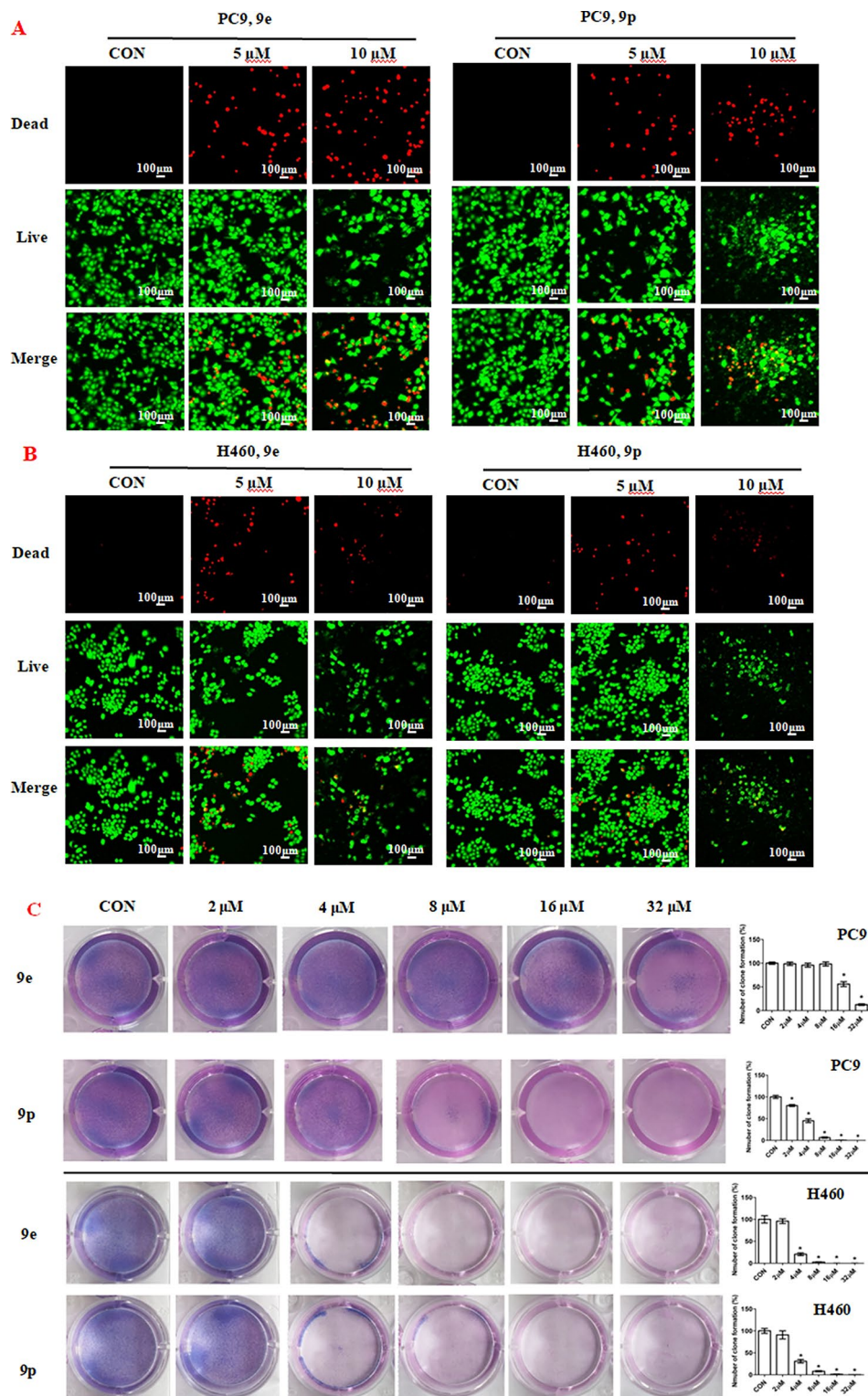


Fig. 2 Inhibition of proliferation of cancer cells by 9e and 9p. **(A)** Fluorescence images stained with the LIVE/DEAD kit of PC-9 cells treated with 5 μ M, 10 μ M and 20 μ M of 9e and 9p. **(B)** Fluorescence images stained with the LIVE/DEAD kit of H460 cells treated with 5 μ M, 10 μ M and 20 μ M of 9e and 9p. **(C)** Plate clone staining of PC-9 cells and H460 cells being treated with different concentrations of 9e and 9p. Data are presented as mean \pm SE. * P <0.05

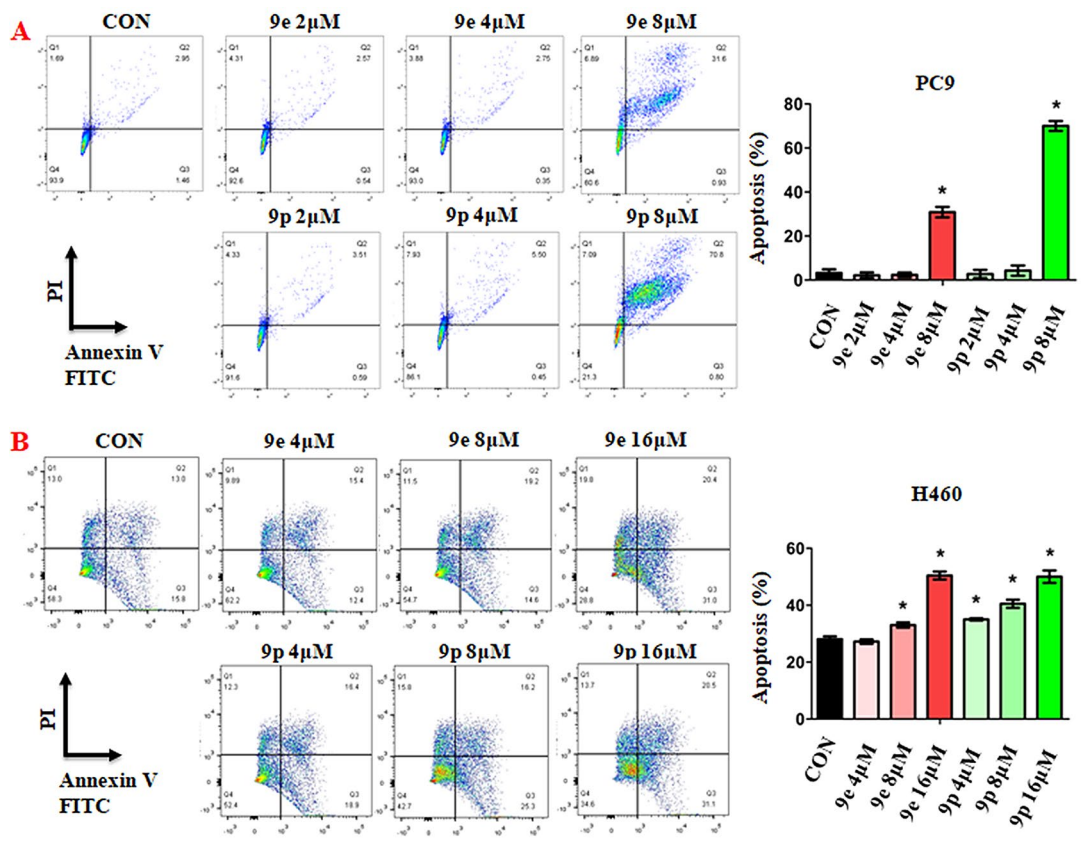


Fig. 3 Apoptosis of cancer cells induced by 9e and 9p. (A) Apoptotic cells of PC-9 cells treated with 9e and 9p determined by flow cytometry. (B) Apoptotic cells of H460 cells treated with 9e and 9p determined by flow cytometry. Data are presented as mean ± SE. *P < 0.05

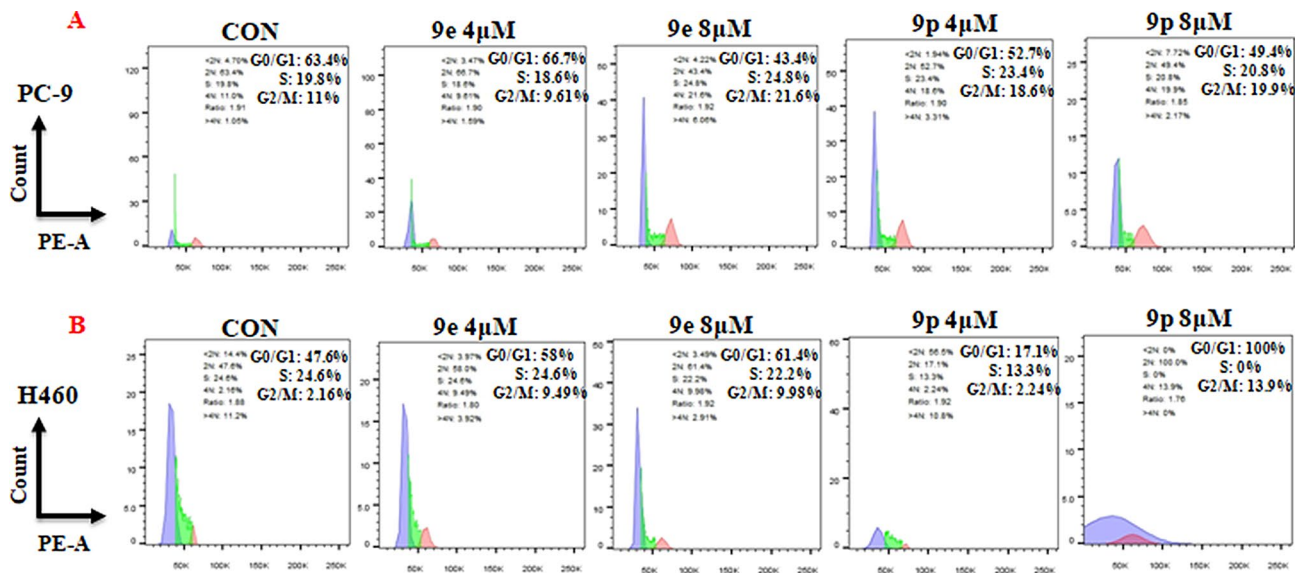


Fig. 4 Influences of 9e and 9p on cell cycles of tumor cells. (A) Flow cytometry analysis of PC-9 cells treated with 9e and 9p compound for 48 h. (B) Flow cytometry analysis of H460 cells treated with 9e and 9p for 48 h. Data are presented as mean ± SE. *P < 0.05

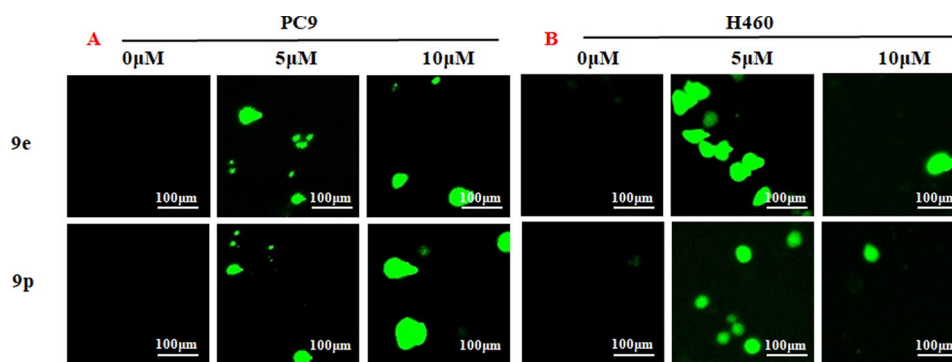


Fig. 5 Compounds 9e and 9p triggered reactive oxygen species generation in tumor cell lines triggered by 9e and 9p. **(A)** ROS detection staining by DCFH-DA in PC-9 cells treated with 9e and 9p at the concentrations of 5 μ M and 10 μ M. **(B)** ROS detection staining by DCFH-DA in H460 cells treated with 9e and 9p at the concentrations of 5 μ M and 10 μ M

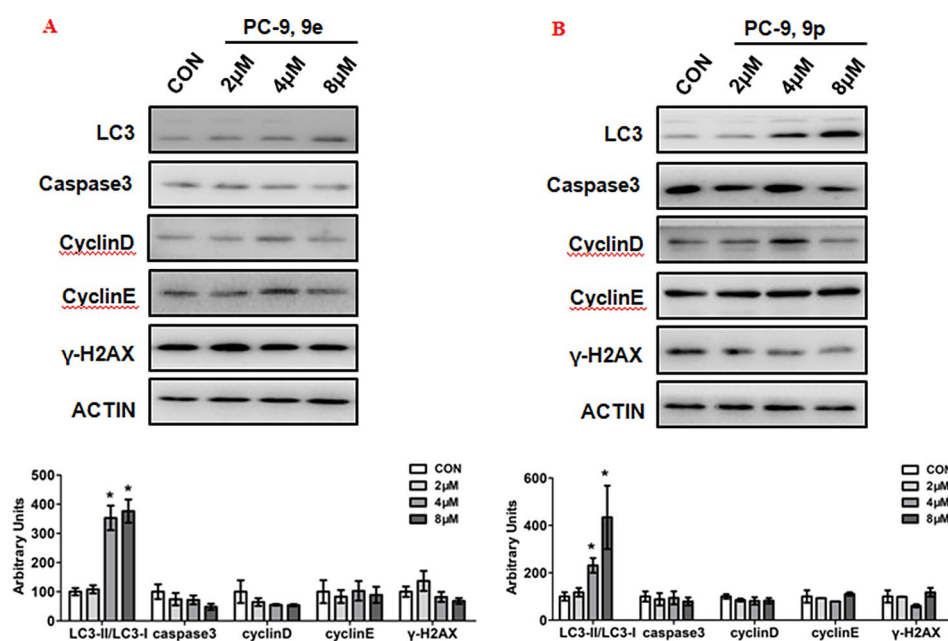


Fig. 6 Influences of 9e and 9p on the expression of key signalling pathway proteins. **(A)** Western blotting of LC3, caspase3, Cyclin D, Cyclin E, γ -H2AX in PC-9 cells treated with 9e. **(B)** Western blotting of caspase3, Cyclin D, Cyclin E, γ -H2AX in PC-9 cells treated with 9p. Top, western blot; bottom, quantitative measurements relative to ACTIN. Data are presented as mean \pm SE. * P < 0.05. The blots were cropped from different parts of the same gel or different gels, and the blots were processed in parallel. The full length original blot was included in the supplementary information

added slowly dropwise in a period of 30 min. The reaction temperature was maintained below 30 $^{\circ}$ C with water bath. After the completion of addition, the reaction mixture was maintained at 10–15 $^{\circ}$ C for another 30 min with the formation of large amount of solid. Methyl tert-butyl ether (100mL) was added, and the suspension was stirred slowly for 15 min. The solid was collected via filtration, was washed twice with methyl t-butyl ether (50mL each), and was dried to give compound 3 as a solid (174 g, 66%). 1 H NMR (400 MHz, DMSO- d_6): δ 10.95 (s, 1H), 7.95 (d, J =16.0 Hz, 1H), 4.56 (s, 2H), 4.40 (t, J^1 =4.0 Hz, J^2 =4.0 Hz, 1H), 3.70 (s, 3 H), 3.45 (s, 3 H), 3.43 (s, 2H), 3.41 (s, 3 H). 13 C NMR (100 MHz, $CDCl_3$): δ 196.89, 166.93, 160.94, 102.73, 98.37, 59.14, 54.91, 51.88, 50.87.

Synthesis of dimethyl 1-(2,2-dimethoxyethyl)-3-methoxy-4-oxo-1,4-dihydropyridine-2,5-dicarboxylate (4)

To a solution of compound 3 (26 g, 0.1 mol) in anhydrous methanol 200mL was added dimethyl oxalate (48 g, 0.4 mol) at room temperature in a period of 30 min with stirring. Sodium methoxide (12 g, 0.22 mol) was added in a rate such that the methanol continues to reflux. The reaction mixture was stirred for 4 h and the course of the reaction was monitored with TLC. After the disappearance of the starting material, the reaction mixture was cooled to 5–10 $^{\circ}$ C. The pH value of the reaction mixture was adjusted to 5–6 with aqueous hydrochloric acid (2 N) and the mixture was maintained at this temperature with a water bath. The solvent was removed in *vasuo*, and the

residue was dissolved in ethyl acetate (1500 mL). The solution was cooled to 10–15 °C, and the pH value was adjusted to 3 with hydrochloric acid (2 N). Water (200 mL) was added, the mixture was stirred, and organic layer was separated. The organic layer was washed with aqueous saturated sodium carbonate to adjust the pH value of organic phase to 8. Finally, 100 mL of water was added, and the organic phases was stirred for 30 min. The organic layer was then separated, and was concentrated to give compound 4 (26.7 g, 81%).

Synthesis of 1-(2,2-dimethoxyethyl)-5-methoxy-6-(methoxycarbonyl)-4-oxo-1,4-dihydropyridine-3-carboxylic acid (5)

A solution of compound 4 (32 g, 0.1 mol) in methanol (150 mL) was added to flask under argon atmosphere. The mixture was cooled to 0 °C with ice-water bath. To this mixture, was added anhydrous LiOH (7.2 g, 0.3 mol) in portions. The solution became turbid during the addition of process of addition of LiOH. The internal temperature of the reaction system was controlled between 0 and 5 °C with ice-water bath. TLC analysis showed the completion of the reaction after 1 h. The pH value was adjusted to 6–7 with slow addition of hydrochloric acid (2 N) at 0–5 °C. Methanol was removed in vacuo. The residue was dissolved with ethyl acetate (200 mL), and the pH value was adjusted to 1–2 via slow addition of hydrochloric acid (2 N). The temperature was maintained at 0 °C during the addition. Organic layer was separated after for 20 min, and the water phase was extracted with ethyl acetate (50 mL × 3). The combined organic layer was washed once with brine (20 mL), and was concentrated to give crude product. Recrystallization of the crude product with methanol gave compound 5 (17.6 g, 59%). ¹H NMR (400 MHz, CDCl₃): δ 8.42 (s, 1H), 4.54 (t, *J*¹=4.0 Hz, *J*²=4.0 Hz, 1H), 4.14 (d, *J*=8.0 Hz, 2H), 4.03 (s, 6 H), 3.42 (s, 6 H). ¹³C NMR (100 MHz, CDCl₃): δ 174.82, 165.83, 161.58, 148.69, 145.25, 136.35, 116.63, 102.27, 60.93, 57.29, 55.89, 53.70.

Synthesis of (4*R*,12*aS*)-7-methoxy-4-methyl-6,8-dioxo-3,4,6,8,12,12*a*-hexahydro-2*H*-pyrido[1';2':4,5]pyrazino[2,1-*b*][1,3]oxazine-9-carboxylic acid (7)

To a reaction flask were added compound 5 (310 g, 1.0 mol) and anhydrous formic acid (1000 mL). The reaction was carried out at 65 °C with stirring under argon atmosphere. The course of the reaction was monitored with TLC. After the completion of the reaction in about 3 h, formic acid was removed in vacuo, and the temperature was kept below 45 °C. The resulting crude oil was re-dissolved in ethyl acetate (300mL), and evaporated again to remove the remaining formic acid. The processes was repeated to ensure that formic acid was removed to the

maximum extent. Finally, compound 6 was obtained with an oil. This oil was used without further purification.

To a solution of compound 6 in acetonitrile (1000 mL) was added (*R*)-3-aminobutanol (125 g, 1.4 mol), and the mixture was stirred for 10 min. The mixture was then heated to reflux for 2.5 h. The course of the reaction was monitored with TLC. After the completion of the reaction, the solvent was removed in vacuo at 40–45 °C. The residue was re-dissolved in dichloromethane (2000 mL). Water (1000mL) was added, and the pH value was adjusted to 1–2 with hydrochloric acid (2 N). The mixture was stirred for 10 min, and the organic layer was separated. The aqueous phase was extracted with dichloromethane (400 mL × 4). The combined organic phase was washed with brine (200 mL × 5), concentrated in vacuo to give crude 7. Recrystallization with methanol gave 7 (225 g,73%). ¹H NMR (400 MHz, CDCl₃): δ 8.43 (s, 1H), 5.30 (t, *J*¹=4.0 Hz, *J*²=4.0 Hz, 1H), 5.02 (t, *J*¹=4.0 Hz, *J*²=8.0 Hz, 1H), 4.41 (dd, *J*¹=4.0 Hz, *J*²=4.0 Hz, 1H), 4.27 (dd, *J*¹=8.0 Hz, *J*²=4.0 Hz, 1H), 4.08 (s, 3 H), 4.03–3.99 (m, 2H), 2.25–2.16 (m, 1H), 1.56 (d, *J*=12.0 Hz, 1H), 1.39 (d, *J*=8.0 Hz, 3 H). ¹³C NMR (100 MHz, CDCl₃): δ 176.39, 165.85, 155.00, 153.90, 142.78, 130.66, 116.08, 75.97, 62.65, 61.48, 53.89, 44.93, 29.37, 16.06.

Preparation of compound 8

In a 500mL reaction flask, 7 (6 g, 0.02 mol), 3-aminophenylacetylene (3.51 g, 0.03 mol), HATU (11.4 g, 0.03 mol), DIPEA (7.8 g, 0.06 mol), and DMF (250mL) were combined at room temperature. The mixture was stirred for 24 h under a nitrogen atmosphere, and the reaction progress was monitored using TLC. Upon completion, confirmed by a light brown color, the reaction solution was poured into 200 mL of water, leading to the precipitation of a solid. The solid was separated, drained, and dried to yield Compound 8 with a 76% yield (6.1 g). ¹H NMR (400 MHz, DMSO-*d*₆) δ 12.55 (s, 1H), 8.70 (s, 1H), 7.96 (s, 1H), 7.60 (d, *J*=8.0 Hz, 1H), 7.38 (t, *J*¹=8.0 Hz, *J*²=8.0 Hz, 1H), 7.22 (d, *J*=8.0 Hz, 1H), 5.39 (dd, *J*¹=4.0 Hz, *J*²=4.0 Hz, 1H), 4.80–4.70 (m, 1H), 4.62 (dd, *J*¹=4.0 Hz, *J*²=4.0 Hz, 1H), 4.40 (dd, *J*¹=8.0 Hz, *J*²=4.0 Hz, 1H), 4.21 (s, 1H), 3.98 (d, *J*=4.0 Hz, 1H), 3.90–3.86 (m, 1H), 3.84 (s, 3 H), 2.09–1.93 (m, 1H), 1.53 (d, *J*=12.0 Hz, 1H), 1.29 (d, *J*=8.0 Hz, 3 H). ¹³C NMR (100 MHz, DMSO-*d*₆): 173.72, 161.81, 155.11, 152.74, 143.11, 138.52, 132.26, 130.35, 129.50, 127.03, 122.46, 122.31, 120.31, 118.59, 117.42, 83.24, 80.78, 75.78, 61.71, 60.21, 52.34, 29.16, 15.67.

General procedure for the preparation of 9 and 10

In a flask, Compound 8 (3 mmol), substituted azide (3.6 mmol), *t*-butanol (75 mL), water (75 mL), tetrahydrofuran (75 mL), copper sulfate (1.2 g, 6 mmol), and sodium ascorbate (0.36 g, 1 mmol) were sequentially added. The

mixture was heated to reflux for 10 h. After completion, the reaction mixture was extracted with dichloromethane (150 mL x 2), and the combined organic layer was washed with brine (50 mL x 4), dried over magnesium sulfate, and concentrated in vacuo to yield the crude product. Recrystallization in ethyl acetate produced the pure compound suitable for further characterization and anti-tumor studies.

The spectroscopic characterization of compounds 9a-9z and 10a-10n is provided as Supporting Information Data.

Biological study

Cell viability assay

CCK8 assay was used to measure cell viability. Cells with a density of 1×10^4 cells/well were seeded on the 96-well plates. After adhesion, cells were treated with different diluted compounds or vehicle control DMSO and continue cultured for 48 h. Then, CCK8 reagent was added for one hour incubation at 37 °C with 5% of CO₂. Absorbance was measured using a microplate spectrophotometer (Thermo) at 450 nm. The ratio of cell viability of control was taken as 100%. For IC₅₀, cells were treated with different concentrations of compounds (0, 0.5 μM, 2 μM, 8 μM, 16 μM, 32 μM) for 48 h and cell viability was determined to calculate the inhibition percentage. Then IC₅₀ of the compounds were investigated using the prism statistical software.

Live and dead cells measurement

PC-9 and H460 cells with a density of 5×10^3 cells/well were seeded on the 96-well plates. Then different concentrations (0, 5 μM, 10 μM, 20 μM) of 9e or 9p were treated for 24 h. Cells were then stained with the LIVE/DEAD Assay Kit, observed and photographed using the fluorescent microscope.

Plate clone formation assay

PC-9 and H460 cells were seeded into 6-well plates at a density of 100–500 cells/well. After 10 days culture, cells were added with 9e or 9p at different concentrations (0, 2 μM, 4 μM, 8 μM, 16 μM, 32 μM) for 48 h. Then cells were fixed by 4% paraformaldehyde and stained by Giemsa dye. An optical microscope was used to photograph cells and count the clone numbers.

Apoptosis assay

PC-9 and H460 cells were cultured in 6-well plates with a density of 3×10^5 cells/well. Different concentrations of 9e or 9p were added to cells for 48 h respectively. The concentrations were 0, 2, 4, and 8 μM for PC-9 cells and 0, 4, 8 and 16 μM for H460 cells. After treatment, Annexin V-FITC Apoptosis Detection Kit was used to determine

the apoptotic ratio and FlowJo software v10 was used to analyze of the results.

Cell cycle assay

PC-9 and H460 cells were cultured in 6-well plates with a density of 3×10^5 cells/well. Cells were treated with different concentrations (0, 4, and 8 μM for PC-9 cells and H460 cells) of 9e or 9p for 48 h respectively. Then the cell cycle was determined by PI staining with the flow cytometer.

Cellular ROS measurement

PC-9 and H460 cells were cultured in 96-well plates in a density of 5×10^3 cells/well. Different concentrations (0, 5 and 10 μM) of 9e or 9p were added to cells respectively for 24 h. After treatment, cells were stimulated with 10 μM DCFH-DA for 30 min at 37 °C, then observed and photographed using a fluorescent microscope.

Western blot

Protein expression levels were measured by western blot. PC-9 cells were cultured in 12-well plates and different concentrations (0, 2, 4, 8 μM) of 9e and 9p were added for 48 h. Proteins were extracted from whole cells using radioimmunoprecipitation assay (RIPA). Buffer containing protease/phosphatase inhibitor cocktail (CST). Sodium dodecyl sulfate (10-15%) polyacrylamide gel electrophoresis and nitrocellulose membranes (Millipore) were used to separate and collect proteins. Antibodies used include, LC3 (3868s, CST), Caspase3 (9662, CST), cyclin D (2922s, CST), cyclin E (20808s, CST), γ-H2AX (9718s, CST), and β-actin (4967s, CST).

Statistical analyses

Data were conducted using Graph pad Prim. A two-tailed Student's t-test or one-way analysis of variance followed by a Student-Newman-Keuls (SNK) test to assess significant differences. Values of $P < 0.05$ were considered statistically significant.

Acknowledgements

Not applicable.

Author contributions

Y.M.L., S.Q.L., and J.X.Y. conceived the study, designed the experiments, and supervised all research. X.X.H. and L.F.M. prepared the draft of manuscript. Y.M.L., S.Q.L., J.X.Y. and H.L.W. revised the manuscript. L.F.M. synthesized all the compounds. X.X.H., L.F.M., L.W. and L.Z.P. carried out the experiments and analyzed the data. All authors reviewed the manuscript.

Funding

This work was supported by National Natural Science Foundation of China (82170606), Basic Research Project of Key Scientific Research Projects of Universities in Henan Province (23ZX006), The Key Scientific Research Projects of Universities in Henan Province (24A350006). The Henan Province Medical Science and Technology Research Project (LHGJ20230450). College Students' Innovative Entrepreneurial Training Plan Program (202310464081). Shenzhen Science and Technology Program (No. JCYJ20210324115208024). International Science and Technology Cooperation Project of Henan Province of China

(242102520016). 2023 Henan Province Central guidance and local science and technology development fund support project(Z20231811030).

Data availability

The data sets used and analyzed during the current study are available from the corresponding author on reasonable request. We have presented all data in the form of Tables and Figure. Dolutegravir-1,2,3-triazole derivatives were synthesized in-house. Dulbecco's modified Eagle medium (DMEM), RPMI 1640 Medium, Fetal bovine serum (FBS) and penicillin/streptomycin were purchased from Gibco (Grand Island, NY, USA). Enhanced Cell Counting Kit-8, Calcein/PI Live/Dead Viability Assay Kit, Giemsa dye and Reactive Oxygen Species (ROS) Assay Kit were obtained from Beyotime Biotechnology (Shanghai, China). Annexin V-FITC/ Propidium iodide (PI) staining kit and Matrigel Matrix were provided by BD Biosciences (Franklin Lake, New Jersey, USA).

Declarations

Ethics approval and consent to participate

Not applicable.

Consent for publication

Not applicable.

Competing interests

The authors declare no competing interests.

Received: 4 June 2023 / Accepted: 29 April 2024

Published online: 07 May 2024

References

- Siegel RL, Miller KD, Wagle NS, Jemal. Cancer statistics, 2023. *CA-A Cancer J Clin.* 2023;73(1):17–48.
- Miller KD, Nogueira L, Devasia T, Mariotto AB, Yabroff KR, Jemal A, Kramer J, Siegel RL. *Cancer Treat Survivorship Stat.* 2022;72(5):409–36.
- Biggar RJ, Chaturvedi AK, Goedert JJ, Engels EA. AIDS-Related cancer and severity of immunosuppression in persons with AIDS. *J Natl Cancer Inst.* 2007;99(12):962.
- Piketty C, Selinger-Leneman H, Bouvier AM, Belot A, Mary-Krause M, Duvivier C, Bonmarchand M, Abramowitz L, Costagliola D, Grabar S. Incidence of HIV-Related anal Cancer remains increased despite long-term combined antiretroviral treatment: results from the French Hospital database on HIV. *J Clin Oncol.* 2012;30(35):4360.
- Atallah-Yunes SA, Murphy DJ, Noy A. HIV-associated Burkitt lymphoma. *Lancet Haematol.* 2020;7(8):594.
- Noy A. HIV Lymphoma and Burkitts Lymphoma. *Cancer J.* 2020;26(3):260.
- Dwivedi P, Kapse A, Bangurwar C, Tamhane A, Banavali. Metronomic Chemotherapy for Burkitt Lymphoma in a patient with HIV: Case Report. *J Pediatr Hematol Oncol.* 2023;45(2):78.
- Lurain K, Ramaswami R, Yarchoan R. The role of viruses in HIV-associated lymphomas. *Semin Hematol.* 2023;59(4):183.
- Pongas GN, Ramos JC. Lymphomas HIV-A. Progress and New challenges. *J Clin Med.* 2022;11(5):1447.
- Zhang C, Xie Q, Hu C. Recent advances in small-molecule HIV-1 integrase inhibitors. *Curr Med Chem.* 2021;28(24):4910.
- Venter WDF, Sokhela S, Net J. Integrase Inhibitors Hand us a New HIV Clinical Puzzle comment. *Lancet HIV.* 2022;9(7):451.
- Klein MB, Young J. Can Integrase Inhibitors Reduce Mortality? *Lancet HIV.* 2022;9(6):371.
- Rabie H. Adult Dolutegravir doses in children. *Lancet HIV.* 2020;7(8):522.
- Nilavar NM, Paranjape AM, Raghavan SC. Biochemical activity of RAGs is impeded by Dolutegravir, an HIV integrase inhibitor. *Cell Death Discovery.* 2020;6:50.
- Nagami EH, Thakarak K, Sax PE. Sustained HIV. Viral suppression with Dolutegravir, Tenofovir, and Emtricitabine as initial therapy despite high-level transmitted Multiclass Resistance. *Open Forum Infect Dis.* 2022;9(2):648.
- Saumoy M, Sanchez-Quesada JL, Ordonez-Llanos J, Podzamczar. Do all integrase strand transfer inhibitors have the same lipid Profile? Review of Randomised controlled trials in naive and switch scenarios in HIV-Infected patients. *J Clin Med.* 2021;10(16):3456.
- Wang WJ, Mao LF, Lai HL, Wang YW, Jiang ZB, Li W, Huang JM, Xie YJ, Xu C, Liu P, Li YM, Leung ELH, Yao XY. Dolutegravir derivative inhibits proliferation and induces apoptosis of non-small cell lung cancer cells via calcium signaling pathway. *Pharmacol Res.* 2020;161:105129.
- Ding Y, Guo H, Ge W, Chen C, Li S, Wang M, Chen Y. Copper(I) oxide nanoparticles catalyzed click chemistry based synthesis of melampomagnonide B-triazole conjugates and their anti-cancer activities. *Eur J Med Chem.* 2018;156:216.
- Kumar PP, Siva B, Rao BV, Kumar GD. Babu. Synthesis and biological evaluation of bergenin-1,2,3-triazole hybrids as novel class of anti-mitotic agents. *Bioorg Chem.* 2019;91:103161.
- Li S, Li XY, Zhang TJ, Mohamed OK. Fan-hao. Design, synthesis and biological evaluation of homoerythrina alkaloid derivatives bearing a triazole moiety as PARP-1 inhibitors and as potential antitumor drugs. *Bioorg Chem.* 2020;94:103385.
- Madasu C, Karri S, Sangaraju R, Sistla R, Uppuluri MV. Synthesis and biological evaluation of some novel 1,2,3-triazole hybrids of myrrhanone B isolated from *Commiphora Mukul* gum resin: identification of potent antiproliferative leads active against prostate cancer cells (PC-3). *Eur J Med Chem.* 2020;188:111974.
- Gupta N, Qayum A, Raina A, Shankar R, Gairola S. Synthesis and biological evaluation of novel bavachinin analogs as anticancer agents. *Eur J Med Chem.* 2018;145:511.
- Emanuela B, Andrea A, Dmitry DZ, Anna PK, Andrea M, Alessandro DL, Murat B, Simone C, Silvia S, Gianluca B, Thomas SP, Marta F, Claudiu TS, Fabrizio. Azidothymidine clicked into 1,2,3-Triazoles: First Report on Carbonic anhydrase-telomerase dual-hybrid inhibitors. *J Med Chem.* 2020;63:7392–409.
- Mao L, Sun G, Zhao J, Xu G, Yuan M. Li. Design, synthesis and antitumor activity of icotinib derivatives. *Bioorg Chem.* 2020;105:104421.
- Ren YL, Lei JT, Zhang TR, Lu P, Cui DD, Yang B, Zhao GY, Peng F, Cao ZX, Peng C. Li. Isobavachalcone, a natural sirtuin 2 inhibitor, exhibits anti-triple-negative breast cancer efficacy in vitro and in vivo. *Phytother Res.* 2024. <https://doi.org/10.1002/ptr.8143>.
- Patil K, Khan AQ, Ahmad F, Kuttikrishnan S, Anver R, Mateo JM, Ahmad A, Bhat AA, Buddenkotte J, Steinhoff M. S. Uddin. Sanguinarine triggers apoptosis in cutaneous squamous cell carcinoma cells through reactive oxygen species-dependent c-Jun N-Terminal kinase signaling pathway. *Front Biosci.* 2021;29(1): 40.

Publisher's Note

Springer Nature remains neutral with regard to jurisdictional claims in published maps and institutional affiliations.